

Supplementary Figure legends

Fig. S1. Schematic representation of the four models used in the regional ABC analysis. Thicker arrows indicate a colonization event. t_0 , time to the last colonization event; t_1 , bottleneck duration; t_c , time between the colonization event and the population recovery (to the current population size, N) after the bottleneck phase.

Fig. S2. Potential distribution of *Cephaloflexa bergi*. (A) Prediction under present day climatic conditions; the colour gradient represents the probability that environmental conditions are suitable for this species. Distribution prediction under the CCSM (B) and MIROC (C) paleo- reconstructed scenarios during the LGM (21 kya); the red colour shows the suitable areas for the species under the 10 percentile training presence criterion (used as threshold). Black dots indicate localities used for the predictions.

Fig. S3. Detailed Bayesian Inference tree for the COI (A) and the ITS-1 (B) data sets, the numbers at the nodes indicate the posterior probability. (C) Neighbor-joining tree inferred from the D_{XY} values of the ITS-1 data. The colour codes correspond to sampling localities as shown in figure 1

Fig. S4. COI Bayesian Inference trees built after removing the most variable positions (5th category). (A) Analyses conducted after removing from the alignment of all sequences those sites that were most variable (5th category) when comparing only the 01-AR population individuals. (B) Analyses conducted after removing from the alignment of all sequences the most variable positions estimated comparing all sequences in the alignment. The sequences of outgroup specimens

F4063, F3952, F2518, F2516 and F2391 are deposited in GenBank under accession numbers KF971679 to KF971683.

Fig. S5: Inference tree inferred to estimate *C. bergi* diversification times. Black spots indicate ancestral nodes for populations (the code is indicated) with two deep lineages (those with descendants in two major clades are represented by big spots). The blue horizontal bar indicates the 95% highest posterior density interval.

Fig. S6. Confusion matrices for the model choice. Bars represent the number pseudo-observed data sets (PODS) generated under the models indicated in the X-axis (true models) and assigned to the LSM (light grey) and LRM (dark grey) models by our model choice procedure.

Fig. S7. Plots comparing the ABC posterior probabilities of the best-supported model in localities 01-AR_1, 04-ED, 07-SO, 10-SB, 13-EC, 19-PC_1, 19-PC_2 and 28-SI_1 with those estimated in sets of 100 discrete bins of probability as in Peter *et al.* (2010) (Empirical probabilities). The probabilities were calibrated as indicated by the dashed lines.

Fig. S8. Truncated prior (black), retained simulations (blue) and posterior density (red) distributions of model parameters under the best-supported model in localities 01-AR_1, 07-SO, 10-SB, 13-EC, 19-PC_1, 19-PC_2. θ , the product of the effective size and the mutation rate ($\theta=4N_eu$) for COI (θ_{COI}) and ITS (θ_{ITS}). c and b , indicate the proportion of the source population that participates in the founding of current sampled SAF populations in the LSM and the LRM models, respectively. T_c and T_b , denote the times of the founding events.

Fig. S9. Distribution of posterior quantiles of true model parameter under the best-supported model in localities 01-AR_1, 07-SO, 10-SB, 13-EC, 19-PC_1, 19-PC_2. p -values of the Kolmogorov-Smirnov test for the uniform distribution are shown on each graph. θ , the product of the effective size and the mutation rate ($\theta=4N_e\mu$) for COI (θ_{COI}) and ITS (θ_{ITS}). c and b , indicate the proportion of the source population that participates in the founding of current sampled SAF populations in the LSM and the LRM models, respectively. T_c and T_b , denote the times of the founding events.

Fig. S1

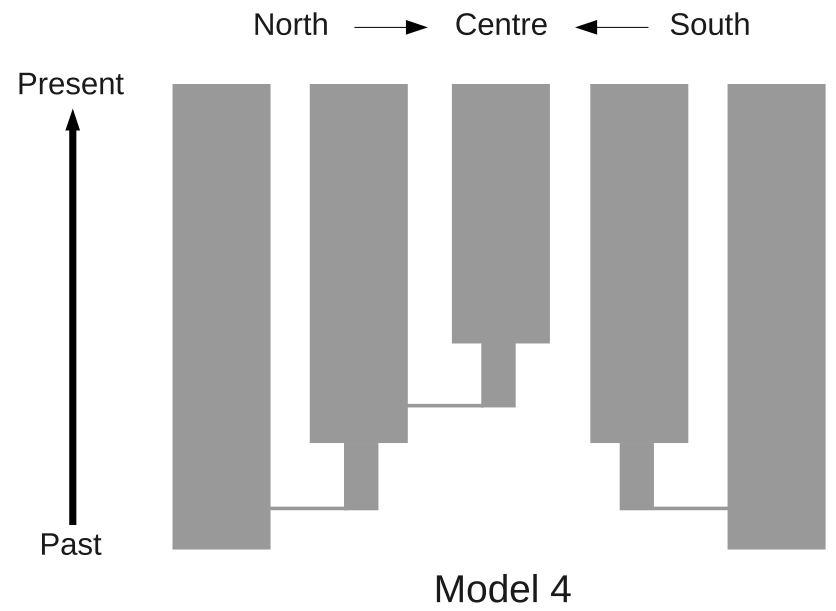
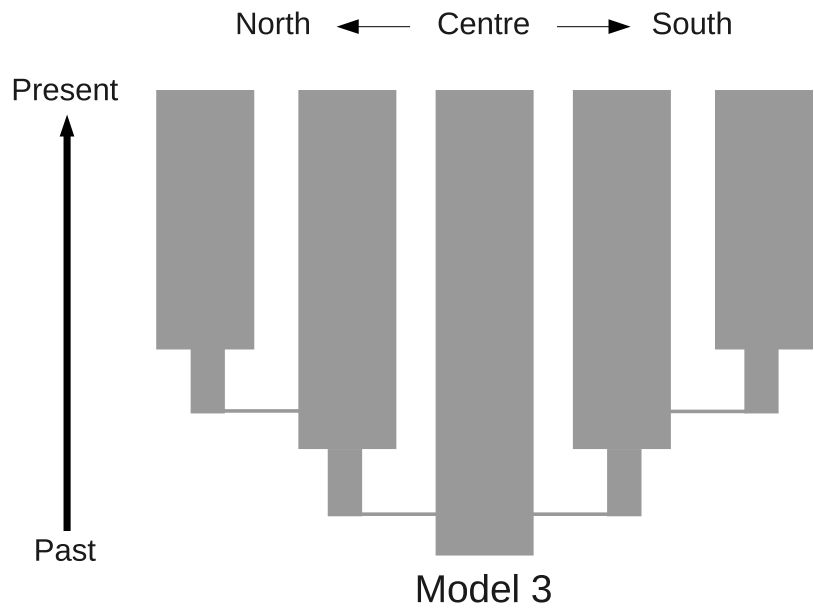
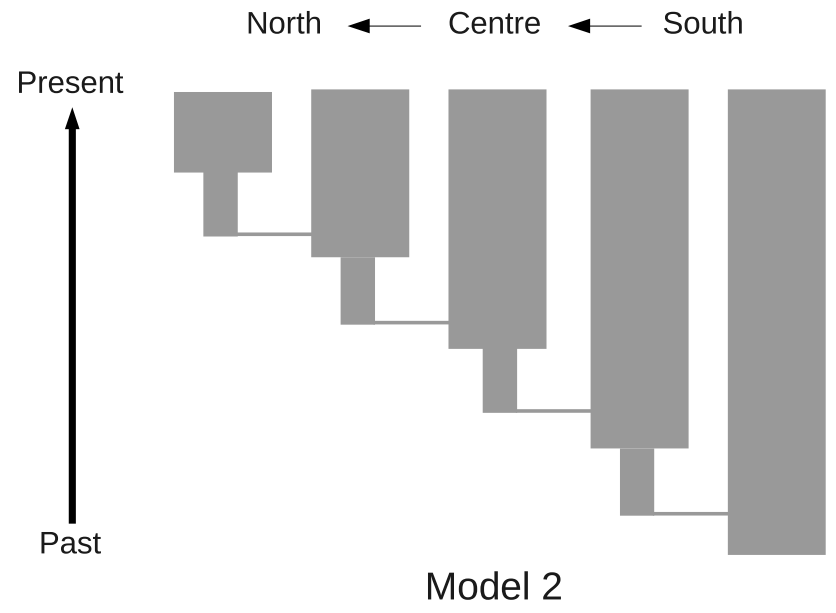
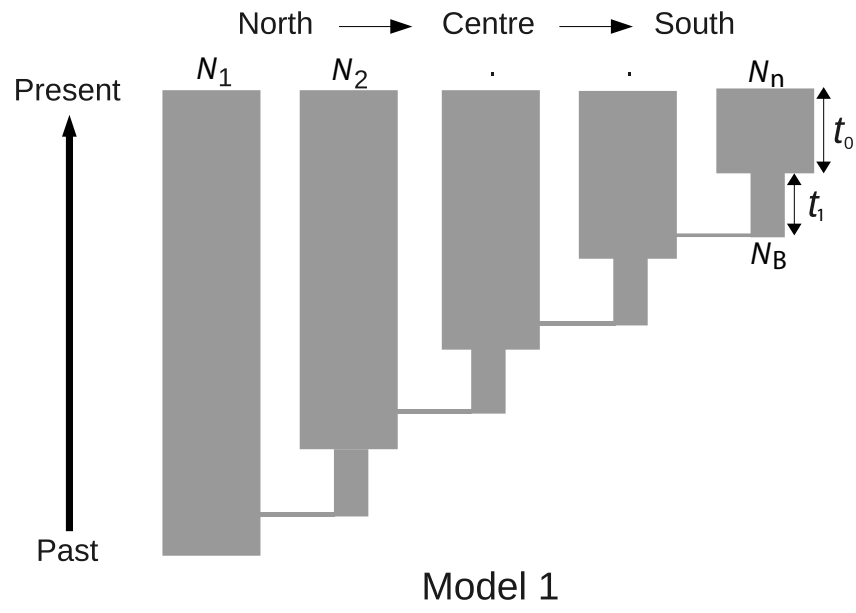
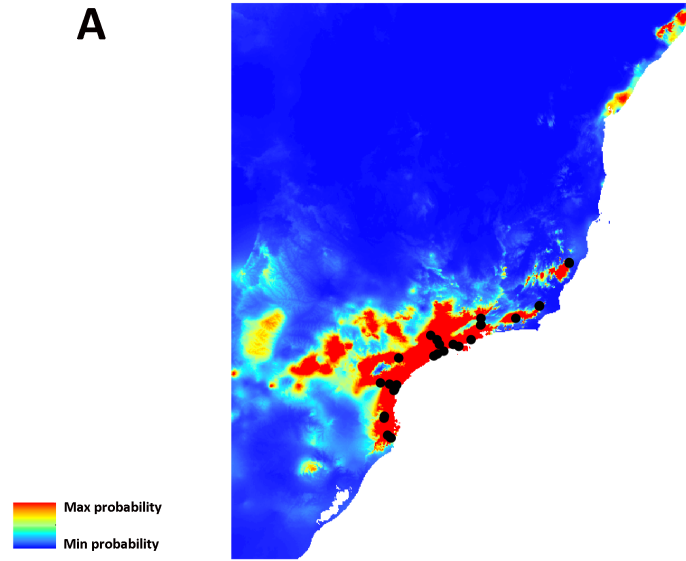
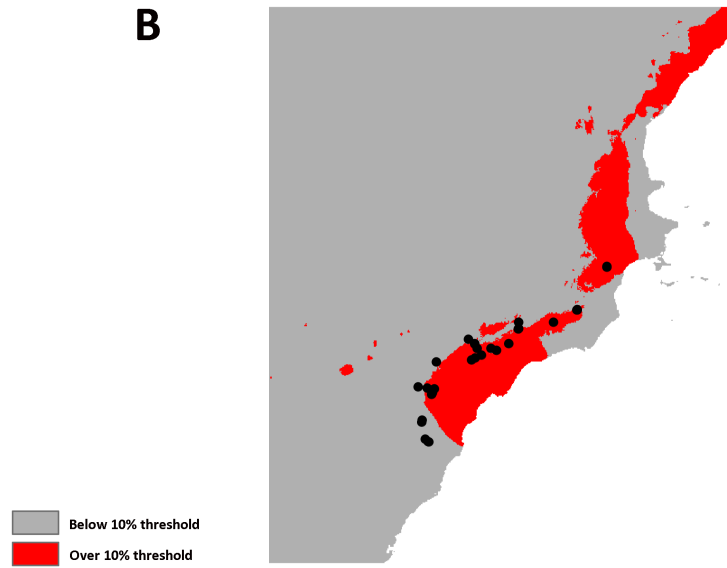


Fig. S2

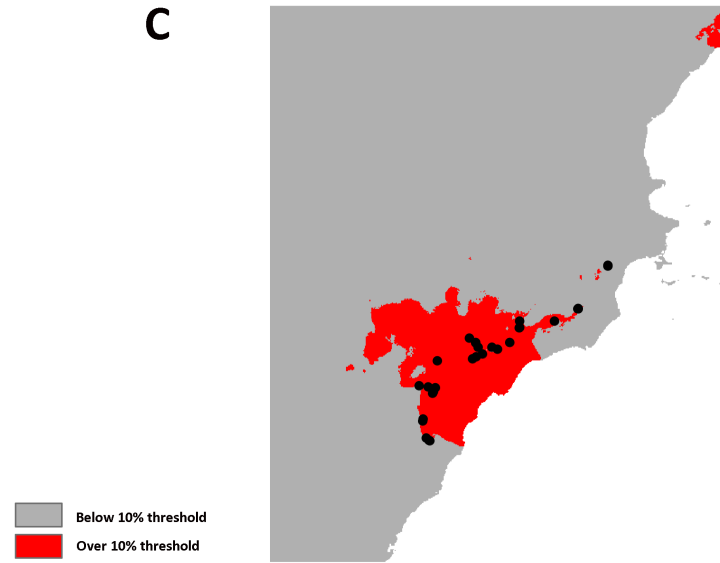
A



B



C



0 1,140 km

A scale bar showing a distance of 1,140 km. The bar is divided into 10 equal segments, with the total length labeled as 1,140 km.

Fig. S3

A



B



Fig. S3

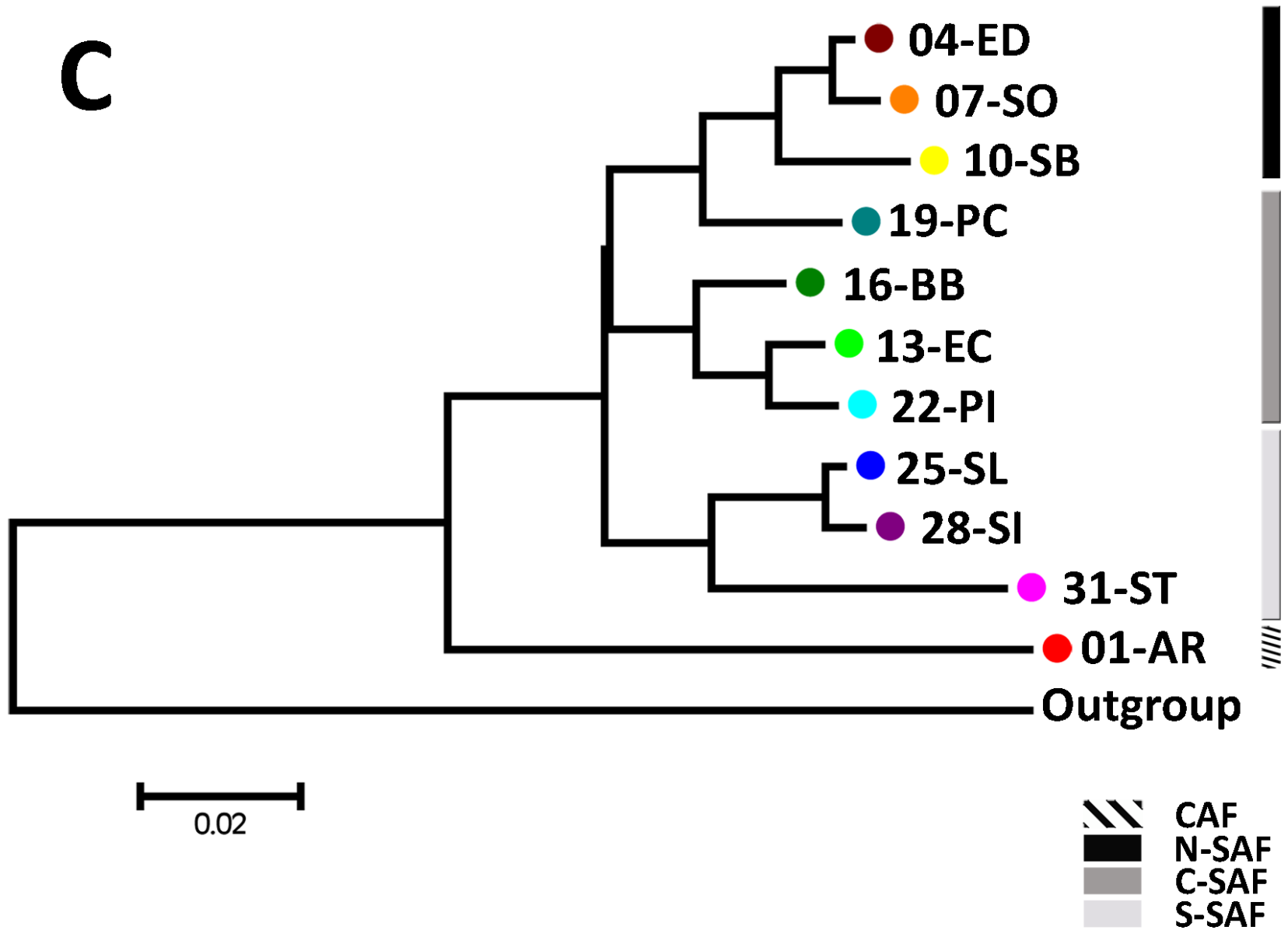


Fig. S5

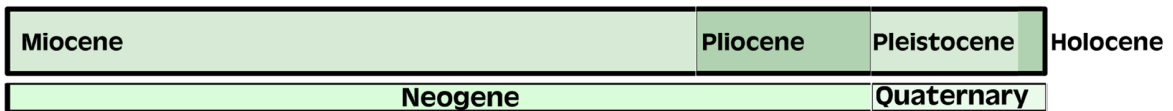
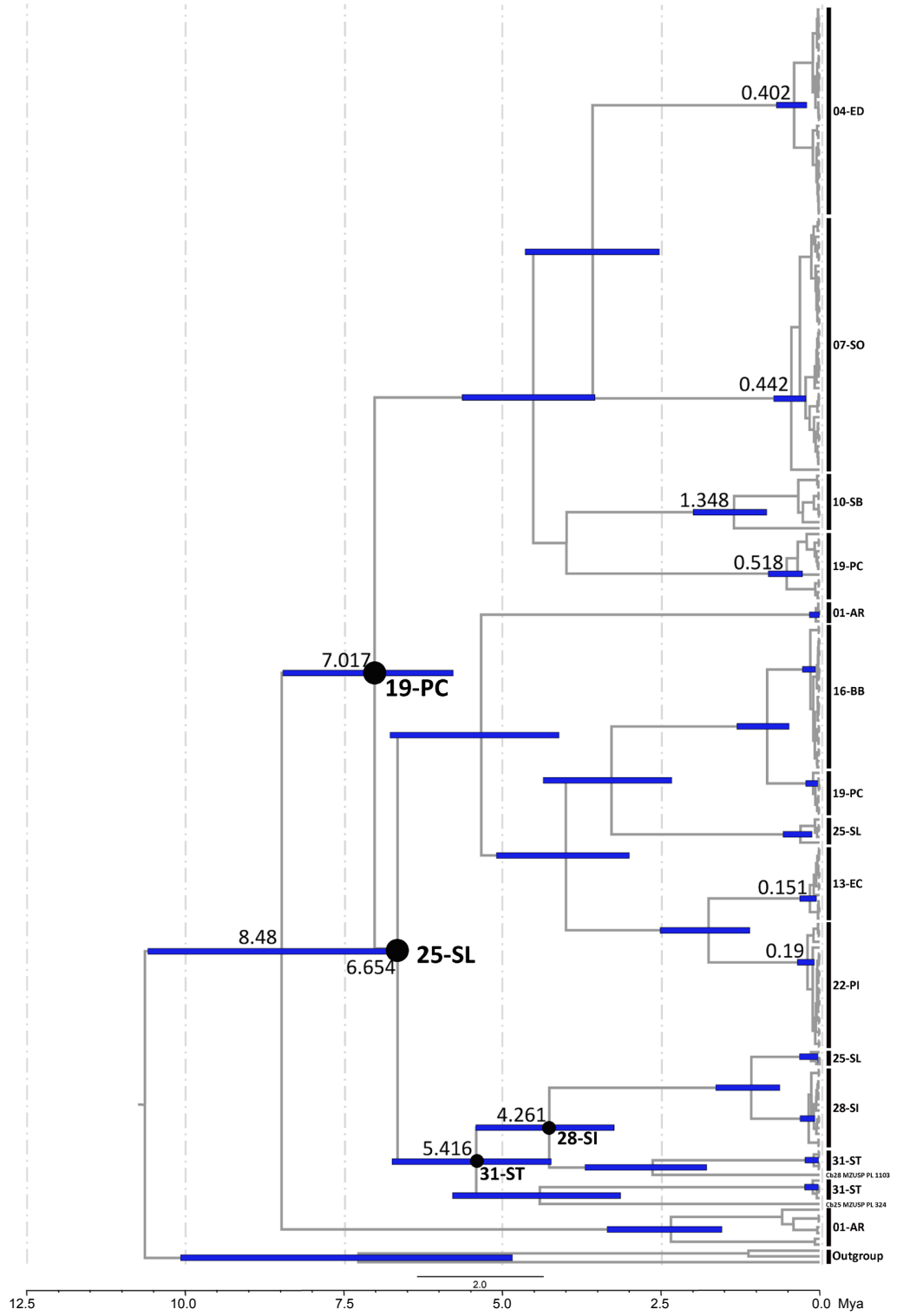


Fig. S6

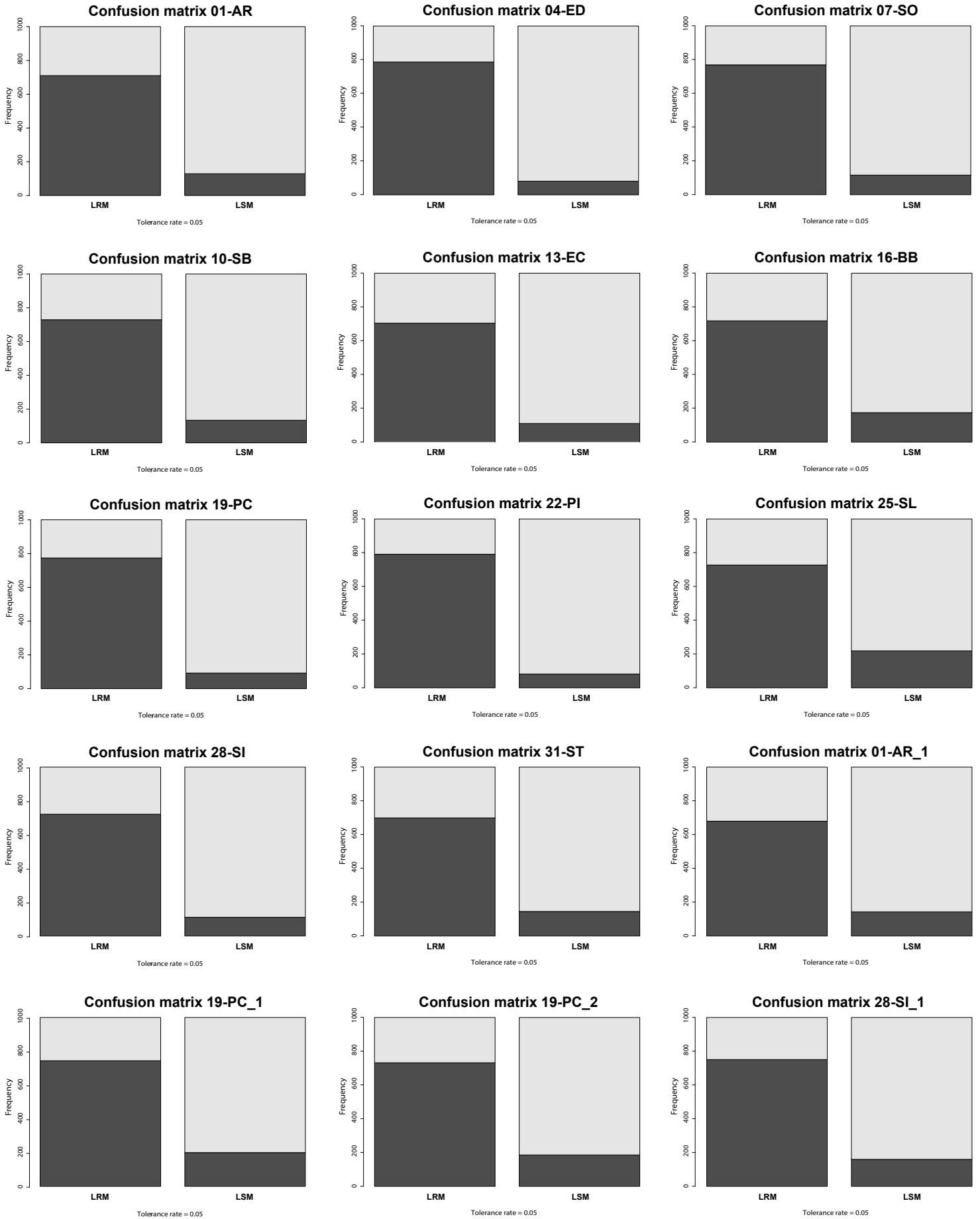
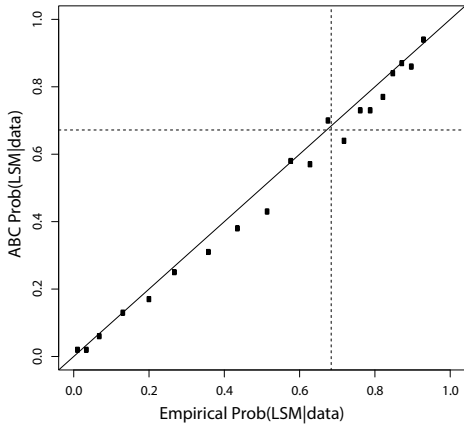
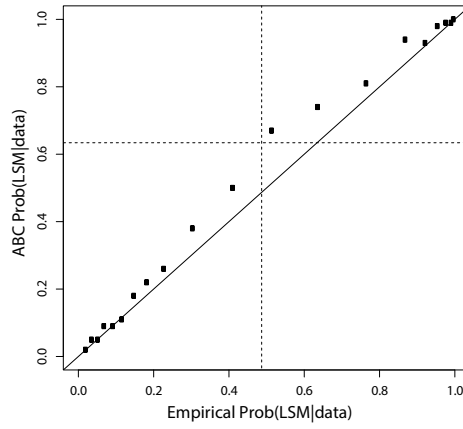


Fig. S7

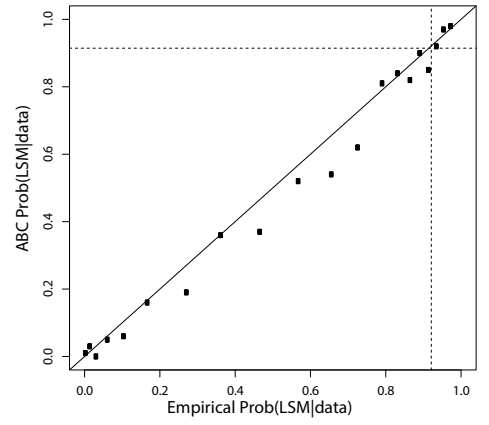
01-AR_1



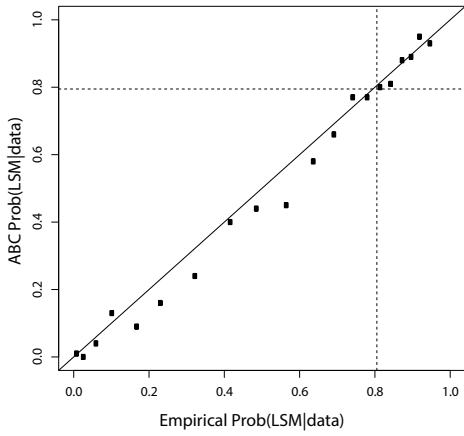
04-ED



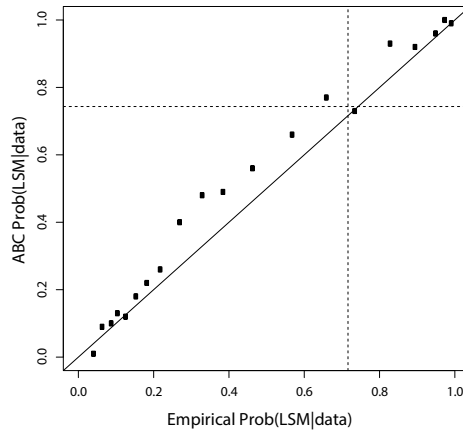
07-SO



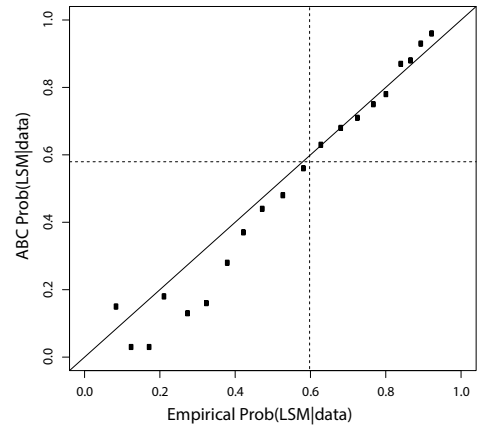
10-SB



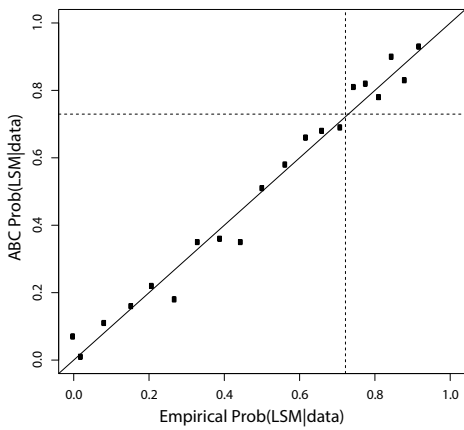
13-EC



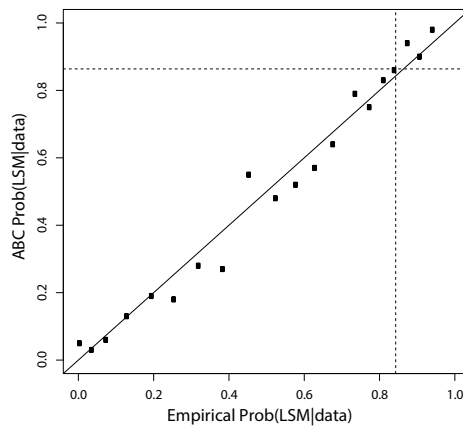
16-BB



19-PC_1



19-PC_2



28-SI_1

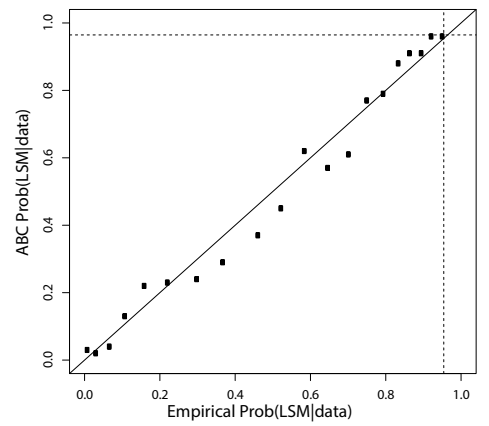


Fig. S8

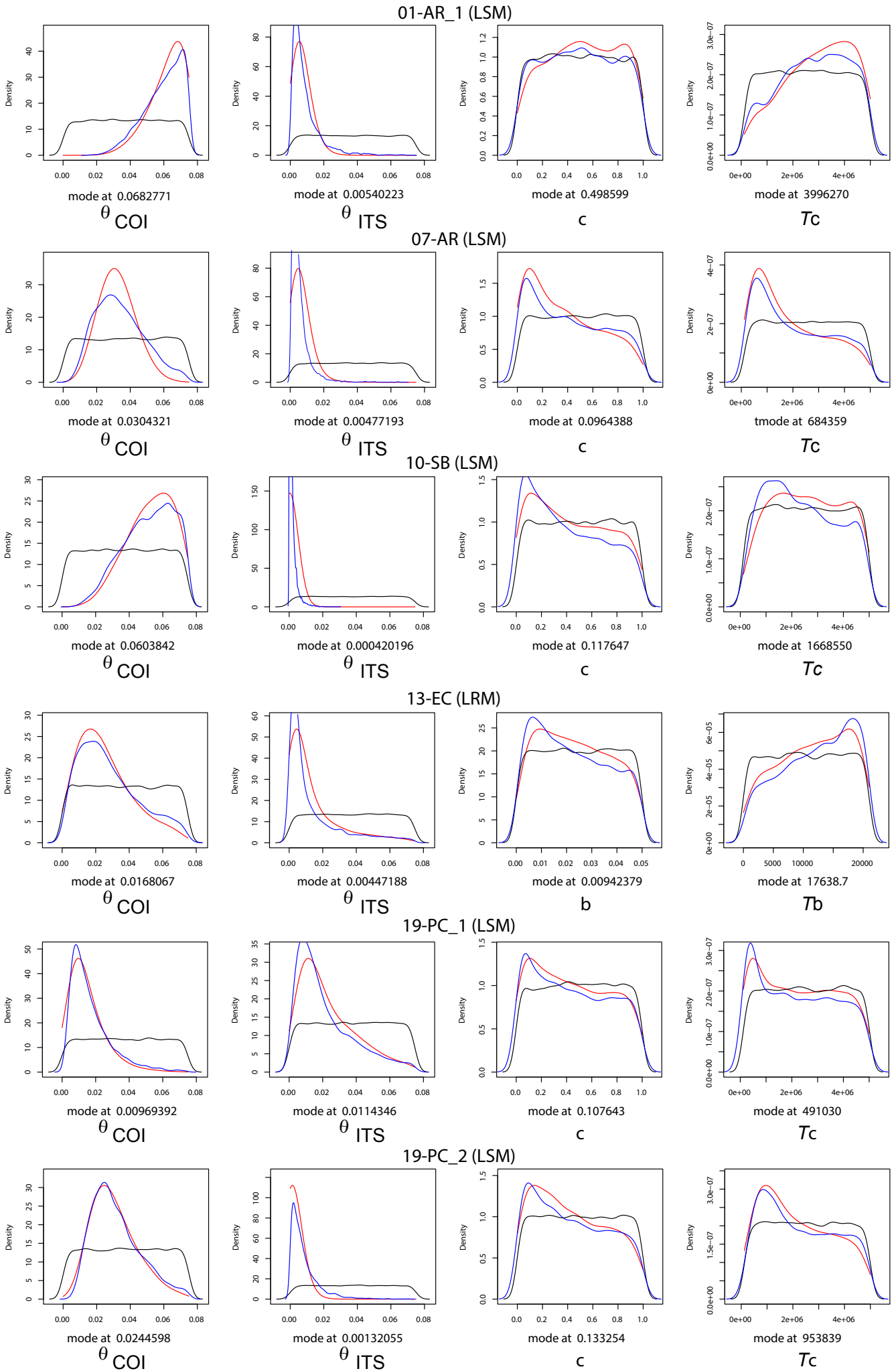
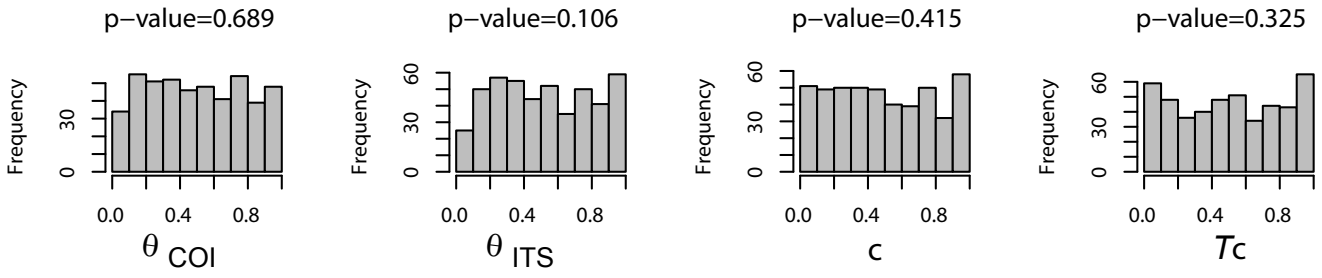
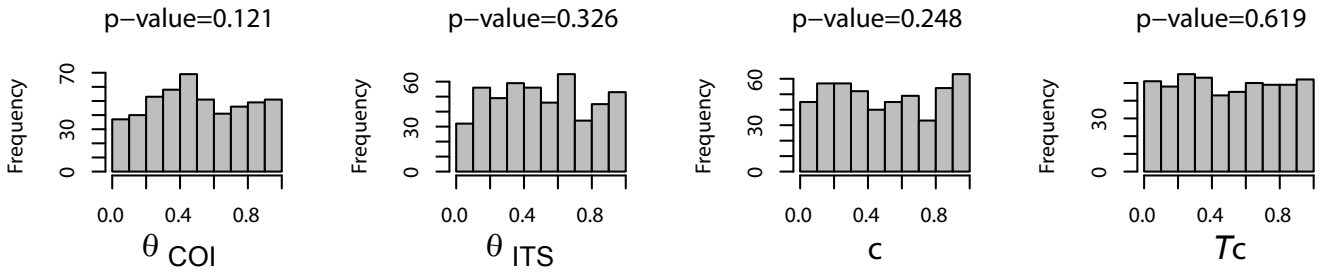


Fig. S9

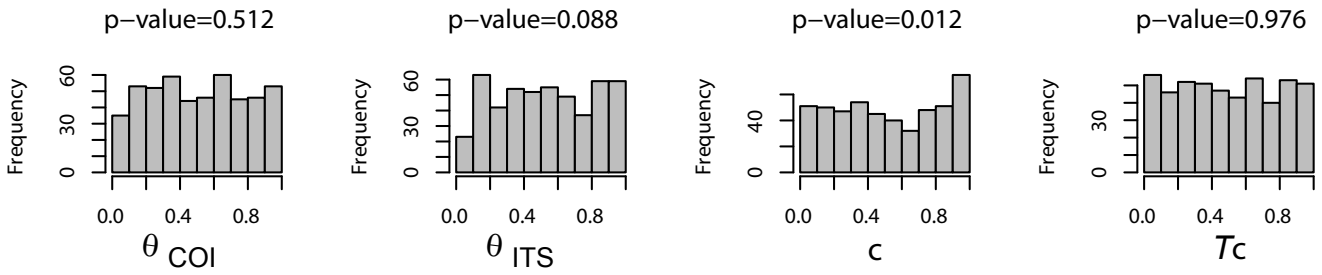
01-AR_1 (LSM)



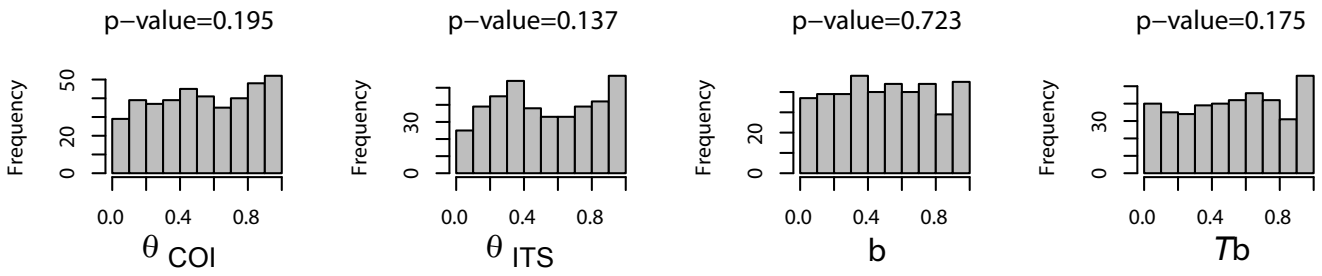
07-AR (LSM)



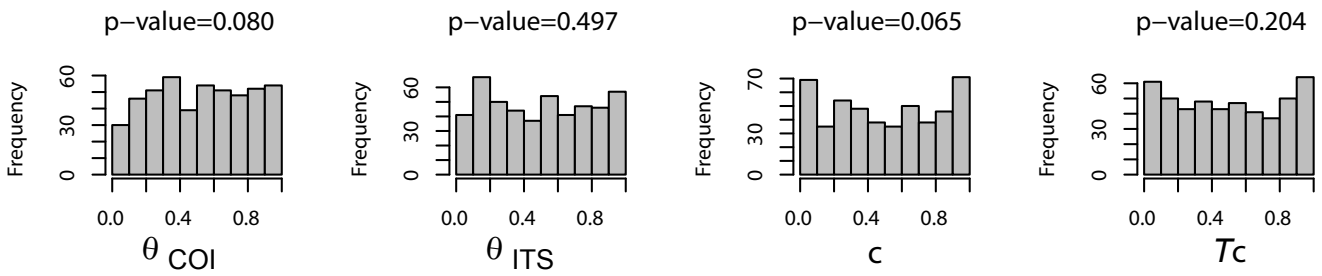
10-SB (LSM)



13-EC (LRM)



19-PC_1 (LSM)



19-PC_2 (LSM)

